Pergamon

PII: S0306-4522(00)00029-4

www.elsevier.com/locate/neuroscience

Neuroscience Vol. 97, No. 2, pp. 227–241, 2000

0306-4522/00 $20.00+0.00

HETEROGENEOUS POPULATIONS OF CELLS MEDIATE SPONTANEOUS SYNCHRONOUS BURSTING IN THE DEVELOPING HIPPOCAMPUS THROUGH A FREQUENCY-DEPENDENT MECHANISM

L. MENENDEZ DE LA PRIDA*§ and J. V. SANCHEZ-ANDRES†‡

*Unidad de Cartografía Cerebral, Instituto Pluridisciplinar, Universidad Complutense, Paseo Juan XXIII, 1, 28040 Madrid, Spain

†Instituto de Bioingeniería, Universidad Miguel Hernández, Campus de San Juan, 03550 Alicante, Spain

‡Departamento de Fisiología, Facultad de Medicina, Universidad de La Laguna, Tenerife, Spain

Abstract—Under normal conditions, hippocampal slices from newborn rats and rabbits (postnatal days 0–8) show spontaneous synchronous bursts known as giant depolarizing potentials. These bursts are recorded from CA3, CA1 and the fascia dentata in both intact slices and isolated hipocampal regions. Giant depolarizing potentials are network-driven events resulting from the synergistic activation of *N*-methyl-D-aspartate, α-amino-3-hydroxy-5-methyl-4-isoxadepropionate and $GABA_A$ receptors, the latter playing an excitatory role. Recently, we showed that they spontaneously emerge in an all-or-none manner after the increase of synaptic and cellular activity beyond a threshold frequency [Menendez de la Prida L. and Sanchez-Andres J. V. (1999) *J. Neurophysiol*. **82,** 202–208]. Under this framework, background levels of spontaneous activity at individual neurons build up network synchronization 100–300 ms prior to the onset of giant depolarizing potentials. However, the role of distinct cellular populations and connectivity in determining the threshold frequency has not been examined. By performing simultaneous intracellular recordings from pyramidal cells, non-pyramidal cells and interneurons, we investigated their participation in the generation of giant depolarizing potentials. Electrodes containing Neurobiotin were used to examine the cellular morphology. We found that giant depolarizing potentials were not initiated from a single pacemaker cellular group; instead, they involved recurrent cooperation among these groups, which contributed differently according to their intrinsic firing capability. In all the neurons examined, the onset of these bursts took place in an all-or-none frequency-dependent manner, both spontaneously (depending on the frequency of the excitatory postsynaptic potentials) or when triggered by extracellular stimulation. The CA3 threshold of frequency was at 12 Hz in both pyramidal cells and interneurons, while in the fascia dentata it was 17 Hz. The application of 6-cyano-7-nitroquinoxaline-2,3-dione increased CA3 threshold of frequency up to 50 Hz, suggesting that it is determined by combined synaptic components. We examined the role of postsynaptic summation on the threshold of frequency. Heterogeneity is present among the cellular groups, pyramidal neurons from CA1 and CA3 showing less evidence of postsynaptic summation prior to giant depolarizing potentials. Cells showing stronger evidence of postsynaptic summation were more typically recorded at the hilus, the granule layer of the fascia dentata and the CA3/CA4 area. Nevertheless, for a given cell, not all the giant depolarizing potentials were preceded by summation of postsynaptic potentials.

These outcomes, together with the long and variable time delays recorded between different areas, strongly suggest that giant depolarizing potentials are locally generated from different initiation sites and not from a single region. We discuss these results in view of the principles underlying hyperexcitability in hippocampal slices, i.e. the intrinsic firing properties of individual cells and the connectivity patterns. © 2000 IBRO. Published by Elsevier Science Ltd.

Key words: slices, intrinsic firing, recurrent loops, synchronization, all-or-none, population bursts.

The idea of a critical period in hippocampal postnatal development characterized by hyperexcitability has received considerable support in recent years. Synchronous bursting is typically recorded from immature hippocampal slices both in control conditions[1,21,40] or when exposed to convulsant drugs,[61] strengthening the view of the hippocampus as a structure susceptible to generate seizures.[59] Attempts to understand the cellular and morphological basis of hippocampal hyperexcitability have been carried out mainly in three *in vitro* configurations: (i) adult hippocampal slices under $GABA_A$ antagonists, such as picrotoxin and bicuculline;[24,48,53] (ii) adult hippocampal slices exposed to 4-aminopyridine or altered ion concentrations, i.e. potassium, magnesium and calcium;[10,28,69] and (iii) immature hippocampal slices exposed to $GABA_A$ antagonists.[61,65] From these experimental studies, as well as from detailed computational models,[71,78] the principles underlying *in vitro* seizure-like discharges can be unified as: (i) the intrinsic firing properties of individual cells that provide background levels of rhythmicity[14,73,74] and (ii) the recurrent excitation that allows rhythmicity to spread and promotes synchrony.[47,72,83]

The spontaneous discharges recorded in immature hippocampal networks (known as giant depolarizing potentials or GDPs) are sustained by excitatory GABAergic transmission also involving synaptic components mediated by *N*-methyl-D-aspartate (NMDA) and α-amino-3-hydroxy-5-methyl-4-isoxadepropionate (AMPA) receptors.[2] Such a heterogeneity in the synaptic components suggests that diverse neuronal populations underlie synchronization in the developing hippocampus.[4,20,34,64] Nevertheless, the role of specific cellular groups (interneurons, pyramidal and non-pyramidal cells)

§To whom correspondence should be addressed. Tel.: +34-91-394-3295; fax: +34-91-394-3264.

E-mail address: liset@eucmax.sim.ucm.es (L. Menendez de la Prida).

Abbreviations: AMPA, α-amino-3-hydroxy-5-methyl-4-isoxadepropionate; CNQX, 6-cyano-7-nitroquinoxaline-2,3-dione; EGTA, ethyleneglycolbis(amino-ethyl ether)tetra-acetate; EPSP, excitatory postsynaptic potential; FD, fascia dentata; GC, granule cell; GDP, giant depolarizing potential; HEPES, *N*-2-hydroxyethylpiperazine-*N*′-ethanesulfonic acid; IB, intrinsic bursting; MC, mossy cell; NMDA, *N*-methyl-D-aspartate; P, postnatal day; SO, stratum oriens; SR, stratum radiatum.

in GDP initiation has not been examined in depth. We have recently demonstrated that GDPs spontaneously emerge in an all-or-none manner after the increase of excitatory postsynaptic potential (EPSP) and cellular activity beyond a frequency threshold.[43] According to this, background levels of unitary activity or EPSPs build up full synchronization in a similar manner as EPSPs and/or electrical activity underlie the initiation of *in vitro* epileptiform bursts.[10,25,28,70] This means a contribution of both intrinsic electrical properties of individual neurons and connectivity patterns to network synchronization, i.e. to GDP generation. Here, we investigate the role of distinct cellular groups (interneurons, pyramidal and nonpyramidal cells) in GDP generation and their participation in determining an appropriate EPSP frequency for synchronization. Portions of this work have been published in abstract form.[42]

EXPERIMENTAL PROCEDURES

Preparation of slices

New Zealand White rabbits (postnatal days P2–P5) and Wistar rats (P1–P6) were killed by decapitation under light ether anesthesia. The whole brain was removed and chilled to 4°C in standard artificial cerebrospinal fluid (composition in mM: 125 NaCl, 3 KCl, 1.2 $MgSO_4$, 1.2 NaH_2PO_4, 2 $CaCl_2$, 22 $NaHCO_3$, 10 glucose, saturated with 95% O_2/5% CO_2, pH 7.4). The hippocampus was dissected from a ventral approach and its dorsal part cut into 500-μm transverse slices with a drop-blade chopper. The slices were maintained in an incubation chamber at room temperature for at least 1 h before recording. For recordings, individual slices were transferred to a submerged-type recording chamber (Medical System) continuously perfused with artificial cerebrospinal fluid at a temperature of 32–34°C (pH 7.4) and a flow rate of 1–1.5 ml/min.

All experiments were carried out in accordance with the protocols approved by Universidad Miguel Hernández and European Communities Council Directive of 24 November 1986 (86/609/EEC). Efforts were made to minimize animal use and suffering.

Intracellular recording and stimulation

Intracellular recording electrodes were made from capillary tubes with intraluminal glass fibers (borosilicate, o.d. 1.2 mm, i.d. 0.69 mm; Sutter Instrument Co.) pulled with a Brown–Flaming horizontal puller (Sutter Instrument Co.), and filled with 3 M KCl (electrode resistances: 50–100 MΩ). Simultaneous intracellular recordings were made with separate manipulators using a dual intracellular amplifier (Axoclamp II B). The intracellular penetrations of CA3 and CA1 neurons were made in the stratum pyramidale. Granule cells (GCs) were impaled at the granular layer. Hilar cells [mossy cells (MCs) and interneurons] were impaled at the hilus. The criteria for a healthy record were a resting membrane potential greater than −50 mV, input resistance larger than 20 MΩ, action potential amplitude greater than 50 mV and a spike response to positive current injection.[58] Experiments under the AMPA/kainate receptor antagonist 6-cyano-7-nitroquinoxaline-2,3-dione (CNQX) were conducted only in rats. Recordings from rat slices were performed in patch-clamp whole-cell configuration (current-clamp mode). Patch electrodes had a resistance of 3–6 MΩ (intracellular solution, in mM: 140 KCl, 1 $MgCl_2$, 1 NaCl, 1 EGTA, 5 HEPES, 2 K_2ATP; pH 7.3, adjusted with KOH). No differences in GDPs were detected between rats and rabbits [a number of experiments ($n = 2$) under CNQX were conducted in the rabbit for comparison; not shown]. Data in Fig. 8 were obtained from rat hippocampal slices.

Electrical stimulation was applied via monopolar tungsten electrodes at the hilus, while intracellular recordings were performed at CA3. The stimulus duration was 100 μs. Ten to 20 trials of periodical stimulation were tested for each frequency value (2–28 Hz).

Dye injection and histology

Neurons were usually injected with Neurobiotin (Vector Laboratories, Burlingame, CA, U.S.A.) for late identification. To achieve this, the tips of the intracellular recording electrodes were filled with 5% Neurobiotin dissolved in 1 M KCl and backfilled with 3 M KCl. Neurobiotin was injected intracellularly using depolarizing pulses (0.2–0.4 nA) at 1 Hz for 10–30 min. After the experiment, the slice was fixed overnight in 4% paraformaldehyde/phosphate-buffered saline (0.1 M, pH 7.4). After H_2O_2 (0.3%) and Triton X-100 (0.6%) pretreatment, the slice was then processed by incubation in a 1:100 dilution of avidin–biotin–peroxidase complex (ABC kit, Vector Laboratories) and by a 0.03% solution of 3,3′-diaminobenzidine and 0.005% H_2O_2. Cells were drawn by a Camera Lucida attachment.

Data analysis

Electrical cell parameters were measured as follows: (i) input resistance was estimated from the I–V relationship near resting potential; (ii) the membrane time constant was calculated from the responses to small hyperpolarizing current pulses (0.1–0.2 nA). Larger pulses were not used because of strong rectification.

EPSP detection was based on the following criteria: (i) only events with amplitude larger than 0.25 mV were counted as EPSPs and (ii) peaks making up clustered events were counted individually if their peak height was greater than the half peak amplitude of the largest. EPSP frequency measured in windows of 500 ms.

The time delay between spontaneous GDPs from simultaneously impaled neurons [CA3–CA1, CA3–fascia dentata (FD)] was defined as the interval between the onset of a GDP in CA3 and the onset of a second GDP. The GDP onset was defined as the peak of the first action potential. We found this to be the most systematic way to define GDP onset. A criterion based on the depolarization underlying a GDP was difficult to apply, since GDP onset was generally masked by EPSPs. Time delay histograms were constructed to investigate the latency distribution between two simultaneously recorded cells. In those histograms, GDP onset in CA3 was taken as a reference. Therefore, positive time delays represent the cases in which CA3 GDPs precede other cell GDPs, as negative time delays represent the cases in which the second impaled neuron (from CA1 or the FD) fires previous to the CA3 cell.

To determine the degree of synchrony between hippocampal areas (CA3, CA1, FD), cross-correlation analyses were applied. The auto- and cross-correlation functions of the membrane potential fluctuations were computed using fast Fourier transform.[51] In the abscissa of these correlograms, function values to the right of zero indicate the cases in which the reference cell (CA3) fires first. The power spectrum from separate signals was also calculated, to assess the frequency components of membrane potential fluctuations from individual cells.[51] Since GDPs appear to involve complex patterns of synchrony between areas CA3, CA1 and the FD,[41] sliding cross-correlograms were computed. A sliding cross-correlogram is a dynamical measure that allows one to investigate detailed temporal characteristic of synchronous signals. To compute this measure, the cross-correlation function from simultaneous recordings in a window of 4 s was calculated. This window was then slid forward by 250 ms and a new cross-correlation function was computed. The cross-correlation function from each sliding window was represented on a color scale from black to yellow. This analysis has advantages over the classical cross-correlation studies[33] by providing a dynamic picture of the entire record.

All the results are given as mean ± S.D.; the number of cells are indicated in every case. Statistical significance analysis using Student's two-tailed t-test was applied (confidence level: $P = 0.05$). Distributions were compared using the Mann–Whitney Rank Sum test. Graphic design was performed with Origin (v. 3.73, Microcal Software).

Materials

The AMPA/kainate antagonist CNQX was purchased from Tocris. Neurobiotin and the ABC kit for 3,3′-diaminobenzidine staining were purchased from Vector Laboratories.

RESULTS

Single cellular populations do not initiate giant depolarizing potentials

As reported previously, spontaneous population bursts or GDPs were recorded systematically *in vitro* from immature hippocampal cells (P2–P5) at a mean frequency of 2.1 ± 1.5 GDPs/min ($n = 43$). GDPs consisted of a large

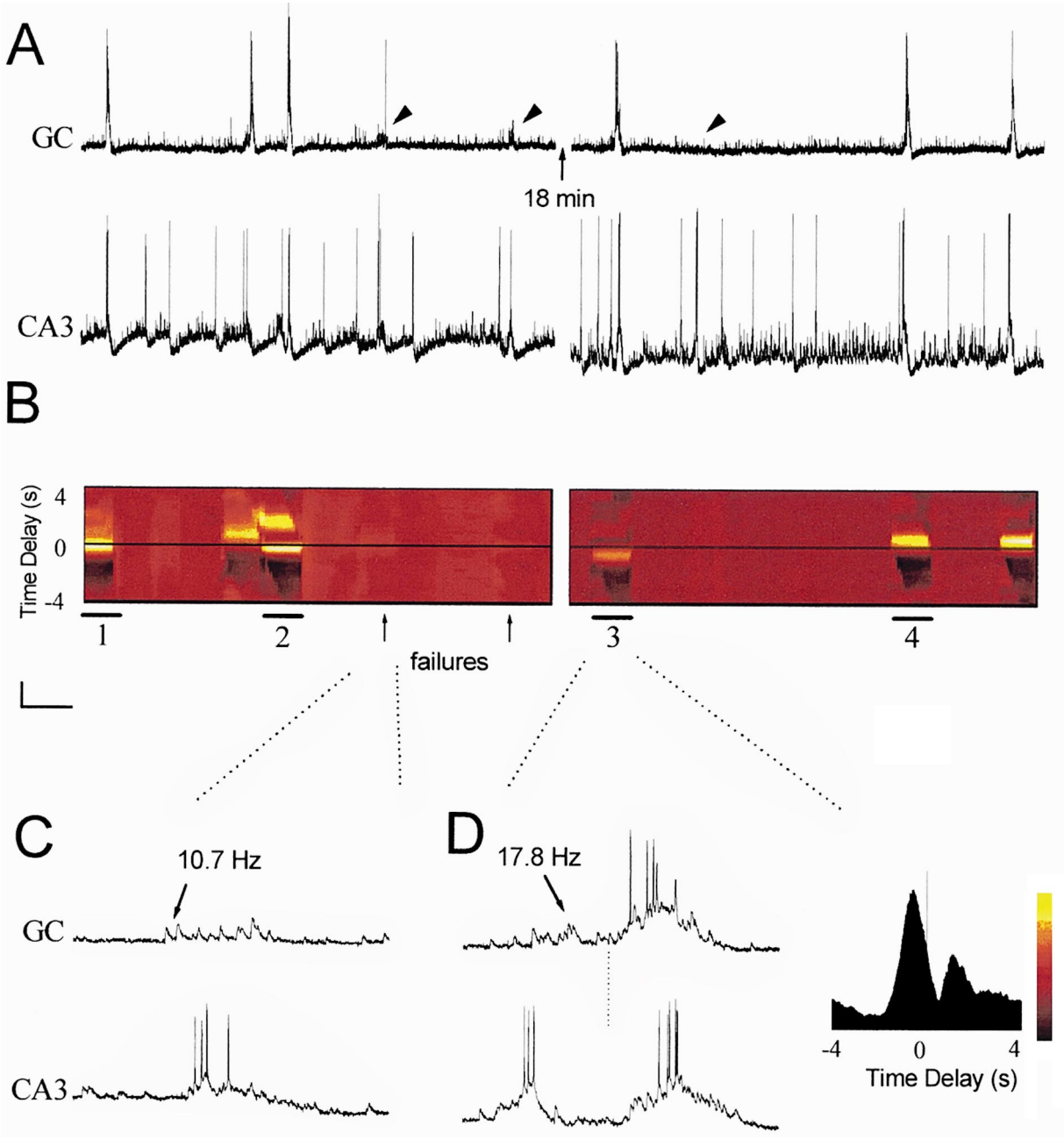

Fig. 1. Simultaneous recordings from granule cells and CA3 pyramidal cells. (A) A GC from the FD was recorded simultaneously to a CA3 pyramidal cell (CA3). GDP frequency was different between these regions, being lower in GCs compared to CA3 neurons. (B) Sliding cross-correlogram from the recordings shown in A. GDPs occurring first in CA3 appeared as maxima (yellow) above the zero line (bar 4). As can be seen, not all the GDPs were first recorded in CA3 cells (bar 1). Double peaks were also detected, indicating the presence of recurrent events (bars 2 and 3). Failures were detected by sliding cross-correlograms, which appeared as small maxima (arrows). (C) Expanded traces showing a failure in GCs. Note the increment of EPSP frequency (13 ± 3 Hz) compared to background levels of EPSPs (4 ± 3 Hz). (D) Double peaks of the sliding cross-correlograms were typical of recurrent events. Here, an increase of EPSPs and firing was recorded at CA3. Then, an EPSP barrage and a GDP were present in GCs, and subsequently recorded at CA3. Note the increase of EPSP frequency prior to GDP onset in both GCs and CA3 neurons. This frequency increment (17 ± 3 Hz) was significantly different from failure. Calibration bars: 20 mV, 2.5 s (A); 20 mV, 250 ms in C and D. Color code shown in B is related to the maxima (yellow) and minima (black) of the cross-correlograms in D (right).

depolarization (21 ± 4 mV) lasting from 190 to 750 ms and crowned by two to seven action potentials (92 GDPs, $n = 21$ cells). GDP reversal potential was -30 ± 10 mV ($n = 8$) and they were blocked by bicuculline (not shown; see Ref. 1).

Simultaneous intracellular recordings from proximal cells (less than 150 μm apart) showed tightly synchronous GDPs, while cells from different areas exhibited long and variable latencies (see Figs 2 and 3 in Ref. 41). Simultaneous recordings from CA3 pyramidals neurons and GCs showed a complex pattern of synchrony ($n = 10$; Fig. 1A). GDP frequency from CA3 neurons was higher (2.9 ± 1.4 GDPs/min) than from GCs (1.5 ± 0.9 GDPs/min). All the GDPs recorded in GCs were correlated with GDPs in CA3 neurons. However, not all the GDPs registered in CA3 were accompanied by a GDP in the GCs, although in these cases an increase in the number of EPSPs was detected (Fig. 1A, arrowheads). We termed these situations as “failures”. A failure occurred when a GDP was detected in one area but failed

Table 1. Summary of the electrophysiological properties of the cells in this study

	CA3 pyramidal $n=43$	CA1 pyramidal $n=35$	Interneurons $n=4$	MCs $N=7$	GCs $n=15$
Resting membrane potential (mV)	-72 ± 5	-69 ± 4	-69 ± 7	-67 ± 3	-66 ± 5
Input resistance (MΩ)	102 ± 25	82 ± 15	72 ± 30	79 ± 11	58 ± 20
Membrane time constant (ms)	21.1 ± 2.2	19.4 ± 2.9	19.0 ± 1.5	20.6 ± 1.5	18.3 ± 2.1
Spontaneous activity (Hz)	0.7 ± 0.6	0.3 ± 0.1	0.8 ± 0.5	1.1 ± 0.9	0.3 ± 0.2
Firing during GDPs (Hz)	17.6 ± 5.1	18.4 ± 4.2	19.6 ± 6.1	19.2 ± 2.8	18.1 ± 3.2

in the other. Failures were more frequent in GCs (9.7%) than in CA3 (2.5%) or CA1 neurons (1.8%).

Typical cross-correlation functions of membrane potential fluctuations from CA3 pyramidal cells and GCs showed a maximum near zero, indicating the occurrence of synchronous events (not shown). In these records, estimation of time delays was difficult due of the large variability present in a given cell pair. Because of the complexity of the firing pattern, we introduced a dynamic measure, i.e. the sliding cross-correlogram, to investigate in detail the temporal relation between the signals (see Experimental Procedures).

The most prominent feature of the sliding cross-correlogram from CA3 pyramidal neurons and GCs was its heterogeneous aspect (Fig. 1B): maxima (yellow) were often found on both sides of the zero line showing negative (see bar 1) and positive (bar 4) time delays. This indicated that, for a given cell pair, synchronous GDPs were not always recorded first in the same neuron. The mean delay between GDPs was 268 ± 101 ms when CA3 cells fired earlier (62.3%) and 221 ± 105 ms when the GDP was first recorded at GCs (results from $n = 10$ sliding cross-correlograms). Sliding correlograms also detected failures of synchronization (Fig. 1B, arrows), which appeared as small maxima (>10% peak amplitude) at the zero line. Failures in GCs were systematically associated with an increase of EPSP frequency (13 ± 3 Hz; Fig. 1C) compared with background EPSPs (4 ± 3 Hz).

Cross-correlation showing two peaks on both sides of the zero line were also detected (bars 2 and 3), indicating the presence of recurrent events. A typical case is shown in Fig. 1D. An increase of EPSPs was recorded in CA3 cells, together with firing. Concomitantly, an EPSP barrage and a GDP were recorded in GCs, which subsequently propagated back to CA3 (dotted line; see cross-correlation function on the right). The EPSP frequency prior to GDP onset was higher (17 ± 3 Hz) than in failures (13 ± 3 Hz; significantly different, $P < 0.001$). This EPSP increment before GDP onset was concomitant with intrinsic bursts (47%; see CA3 cell in Fig. 1D) or single spikes (39%), suggesting a role of the intrinsic firing properties in GDP generation.

Similar results were obtained from CA3 and CA1 pyramidal cells, i.e. positive and negative GDP delays and double peaks in the sliding cross-correlograms ($n = 10$ sliding cross-correlograms; not shown), together with EPSP and spike barrages prior to GDP onset.

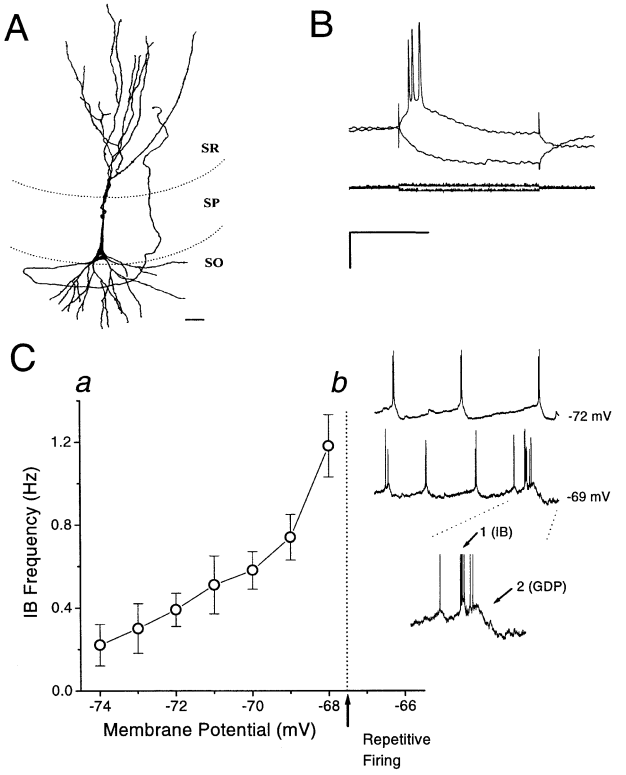

Fig. 2. Intrinsically bursting CA3 pyramidal cells. (A) Camera Lucida drawing of a CA3 pyramidal cell which showed intrinsic bursting activity. These cells constituted 40% of the CA3 population of pyramidal neurons. Scale bar = 25 μm. (B) Response of the cell shown in A to depolarizing and hyperpolarizing current pulses of ±0.1 nA. (Ca) Dependence of the frequency of intrinsic bursting against the membrane potential ($n = 5$). Depolarization beyond −68 mV switched the firing mode from intrinsic bursting to repetitive firing (vertical arrow and dotted line). (Cb) Spontaneous rhythmic activity recorded from the cell shown in A. Expanded trace, IB activity (arrow 1 in −69 mV trace) was recorded prior to GDPs (arrow 2) concomitant to EPSP barrage in 47% of cases. Calibration bars: 20 mV, 200 ms (B); 25 mV, 1.5 s (Cb).

Simultaneous recordings from heterogeneous populations of CA3 pyramidal cells reveal heterogeneity during giant depolarizing potentials

To investigate the cellular and network mechanisms underlying GDP generation, we have recorded from different cellular populations. The electrophysiological properties of the cells examined in this study are summarized in Table 1.

Intracellular recordings from CA3 pyramidal cells revealed large electrophysiological heterogeneities. About 40% of the CA3 pyramidal cells showed intrinsic bursting (IB) activity. They were pyramidal-shaped neurons ($n = 17$; Fig. 2A) showing: (i) a single burst as a response to depolarizing current pulses (Fig. 2B) and (ii) spontaneous rhythmic IB activity depending on membrane potential (Fig. 2Ca). These cells fired intrinsic bursts at frequencies from 0.2 to 1.2 Hz when membrane potential was set at different values ranging from −74 to −68 mV.[82] Depolarization beyond -68 ± 2 mV switched the firing mode from IB to repetitive firing at

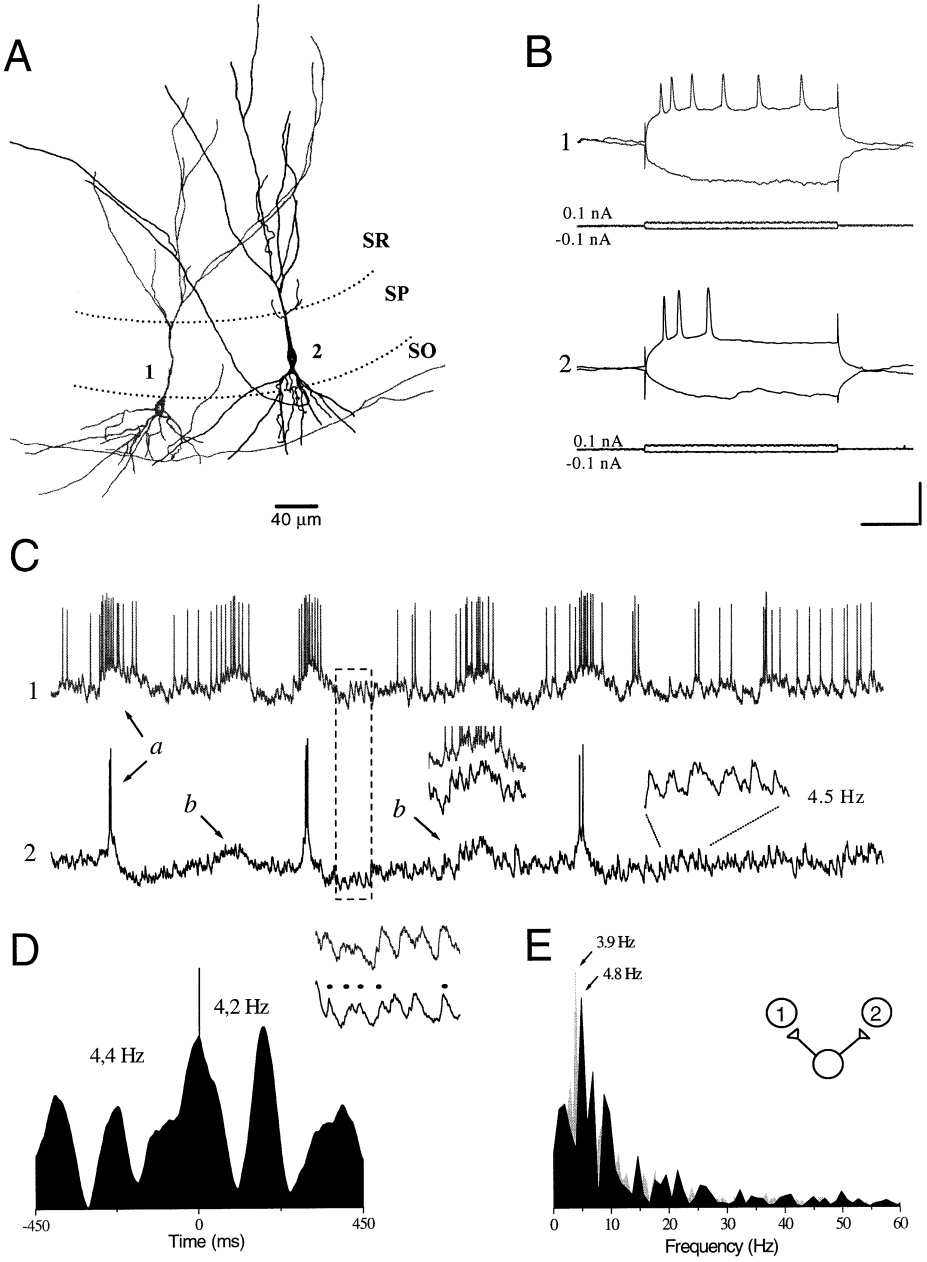

Fig. 3. Simultaneous recordings from two CA3 pyramidal cells. (A) Camera Lucida drawing of the neurons recorded simultaneously. Scale bar = 40 μm. (B) Responses of the cells shown in A to depolarizing and hyperpolarizing current pulses of ±0.1 nA. Cell 1 showed a non-stereotyped firing pattern while cell 2 responded with a burst of action potentials. (C) Simultaneous recordings from cells shown in A. Note the difference in the firing pattern during GDPs (arrow a). Low percentages of failures were recorded in CA3 cells (1%, arrow b and expanded traces). (D) Synchronous spontaneous EPSPs were detected in a number of simultaneous recordings from CA3 pyramidal cells ($n = 5$). See square in C and expanded traces in D, right. Classical cross-correlation function of the membrane potential fluctuations from these records showed multiple peaks consistent with a rhythmic behavior from 1 to 5 Hz. (E) Power spectra from membrane potential fluctuations from proximal cells confirmed the presence of similar frequency components. Data from cells 1 and 2 are represented (3.9 and 4.8 Hz, respectively). These data suggest that cells 1 and 2 received divergent synapses from rhythmically presynaptic neurons (see schematic representation on the right). Calibration bars: 30 mV, 100 ms (B); 25 mV, 300 ms (C); 4 mV, 20 ms (D).

5.2 ± 2.1 Hz. This voltage dependency caused strong changes in the individual firing patterns, since spontaneous small membrane potential variations such as 3-mV depolarization were able to modulate IB frequency (Fig. 2Cb). As shown in Fig. 1D, IB activity was present concomitantly with the EPSP increase recorded 100–300 ms prior to GDP onset in 47% cases (data from 588 GDPs), suggesting that this rhythmic firing may contribute to GDP generation (Fig. 2Cb, expanded trace, arrows 1 and 2).

Some pyramidal cells (non-IB cells, $n = 21$, 48%) did not show spontaneous rhythmic IB activity depending on membrane potential, although their responses to depolarizing pulses consisted of a single burst of action potentials similar to IB cells (cell 2 in Fig. 3A, B). On the other hand, a small population of pyramidal cells did not show a stereotyped behavior (non-stereotyped cells, $n = 5$, 12%). Some of these cells ($n = 3$) had their somas located out of the stratum pyramidale (Fig. 3A, cell 1). Their responses to depolarizing current pulses were not stereotyped (Fig. 3B). Spontaneous activity also reflected this heterogeneity, from silent

($n=2$ cells) to spiking activity in the range of 3–10 Hz ($n=3$).

Simultaneous recordings from CA3 pyramidal cells evidenced their different behavior during GDPs. IB cells fired mixed intrinsic bursts and action potentials at high frequencies (21.9 ± 5.6 Hz) during GDPs (see Fig. 2Cb, arrows 1 and 2). On the contrary, non-IB cells contributed diversely to GDPs. Ninety percent of these cells fired action potentials (18.4 ± 7.2 Hz) during the entire depolarization underlying GDPs (Fig. 3C, cell 1, arrow a), while others fired two to three high-frequency spikes (36.7 ± 8.8 Hz) just at GDP onset (Fig. 3C, cell 2, arrow a). The majority of pyramidal cells (~60%) showed spontaneous activity and increased their firing frequency prior to GDP onset. Local failures were recorded in few cases (1%; Fig. 3C, arrow b and expanded traces). The spiking frequency in these cases (15.4 ± 4.8 Hz) was not significantly different from that recorded during GDPs ($P > 0.001$), suggesting that a single pyramidal cell was not able to generate them.

In a number of paired recordings we found evidence of synchronous spontaneous EPSPs ($n=5$; see square in Fig. 3C, and expanded traces in Fig. 3D). The occurrence of these events was not dependent on membrane potential, suggesting a synaptic source. Classical cross-correlation functions of the membrane potential fluctuations from these recordings showed multiple peaks consistent with a rhythmic and synchronous activity in the range from 1.5 to 5 Hz (Fig. 3D). Power spectra from fluctuations of spontaneous synaptic activity from proximal cells confirmed the presence of similar frequency components (Fig. 3E, spectra from cells 1 and 2 are represented), suggesting, in these cases, that simultaneously recorded cells received a common input from a rhythmic presynaptic cell (see schematic diagram in Fig. 3E, right).

Interneurons fire at high frequency during giant depolarizing potentials

Intracellular recordings from interneurons revealed that they fired at high frequency (12–45 Hz) and showed multiple EPSPs during GDP firing. Figure 4A shows a CA3 interneuron with its soma placed at the stratum radiatum (CA3/SR interneuron). This interneuron was recorded simultaneously to a CA3 pyramidal cell (Fig. 4C). As can be seen, high-frequency spiking and multiple EPSPs were present at the interneuron during GDPs (see square). The results of EPSP frequency in interneurons are summarized in Fig. 4D. EPSP frequency during GDPs (gray histogram) could be well fitted by a Gaussian distribution centered at 29.1 ± 3.9 Hz, which differed significantly from the background EPSP distribution (noise, white histogram; 4.3 ± 2.5 Hz; $P < 0.001$). In the interneurons, the frequency of the action potentials during GDPs did not follow a Gaussian distribution; instead, three peaks were identified (Fig. 4D, black histogram). The first peak (17.1 ± 7.5 Hz) corresponded to low-frequency spikes (see asterisk in Fig. 4D, inset a). The second peak (33.4 ± 6.1 Hz) was not significantly different from the EPSP distribution (29.1 ± 3.9 Hz; $P > 0.001$; gray histogram and see filled square in inset a, Fig. 4D). The third peak (42.7 ± 5.1 Hz) corresponded to high-frequency spikes, such as doublets (filled circle), and first-order spikes, i.e. the first spikes of a GDP (see open square, inset b, Fig. 4D).

Simultaneous recordings from CA3 interneurons ($n=3$) and cells from the FD (MCs or GCs) showed variable time delays, as described above for CA3 pyramidal and granule cells. A simultaneous recording from the interneuron in Fig. 4A (cell 1) and an MC (cell 3) is shown in Fig. 4E (top). Time delay histograms from the interneuron and the MC showed that there were few cases in which the interneuron fired first (time delays >0; Fig. 4E, top, F). Sliding cross-correlograms from paired recordings from CA3 interneurons and FD cells showed a delay of 180 ± 24 ms when FD cells fired first and 189 ± 28 ms when GDPs were first recorded in the CA3 interneuron. Similarly, in simultaneous recordings from CA3 interneurons and CA1 pyramidal cells (Fig. 4E, bottom), the time delay histograms showed large variability ($n=3$ simultaneous recordings; see Fig. 4F): 152 ± 41 ms when GDPs were first recorded at CA3 interneurons and 197 ± 22 ms in cases where the CA1 cell fired first.

Frequency dependence of the initiation of giant depolarizing potentials in CA3 interneurons, CA3 pyramidal cells and granule cells

The results discussed above suggest a different cellular contribution to GDP generation according to the intrinsic firing properties. Nevertheless, in all the cases a relationship between the EPSP frequency and GDP occurrence can be proposed. As reported previously, an all-or-none dependence between EPSPs and GDP onset has been demonstrated in CA3 pyramidal cells.[43] It is therefore important to investigate the frequency dependence of GDP initiation in CA3 interneurons compared to CA3 pyramidal cells and neurons from the FD.

Mossy fiber stimulation-evoked GDPs in CA3 interneurons and pyramidal cells in a process depending on the stimulation frequency (Fig. 5A, open circles show data from $n=3$ interneurons and black squares data summarized from $n=12$ pyramidal cells), similarly as they originated spontaneously from EPSP accumulation in the FD (Fig. 5A, gray squares). To compute these curves, extracellular stimulation of minimal strength was applied at several frequencies (1–20 Hz) and the amplitude of the evoked GDP was calculated. In cases where no GDP was evoked, its amplitude was taken as zero. The curve from spontaneous GDP initiation in FD cells was calculated by analysing failures in CA3–FD recordings: EPSP frequency during a failure was associated with a zero-amplitude GDP, while EPSP frequency prior to GDP onset was represented together with the GDP amplitude ($n=9$). The GDP threshold was defined at the 50% level of the mean normalized amplitude. GDP threshold in the CA3 interneurons was at 12.5 Hz and in pyramidal cells was at 11.8 Hz. In granule cells from the FD, the GDP threshold was at 17.6 Hz.

Figure 5C shows the results obtained in a CA3 interneuron which its soma placed at the stratum oriens (SO; Fig. 5B). Repetitive stimulation at 1–8 Hz did not induce GDPs irrespective of the stimulus duration. On the contrary, GDPs were fired by repetitive stimulus above 12 Hz. Figure 5C shows a spontaneous (a) and an evoked GDP (b) recorded from the interneuron shown in Fig. 5B. Trace b shows a typical case of the effect of mossy fiber stimulation over the CA3 interneurons. The first four stimulations evoked action potentials in the CA3/SO interneuron. GDPs emerged afterwards (vertical arrow). Data from interneurons suggest that GDPs

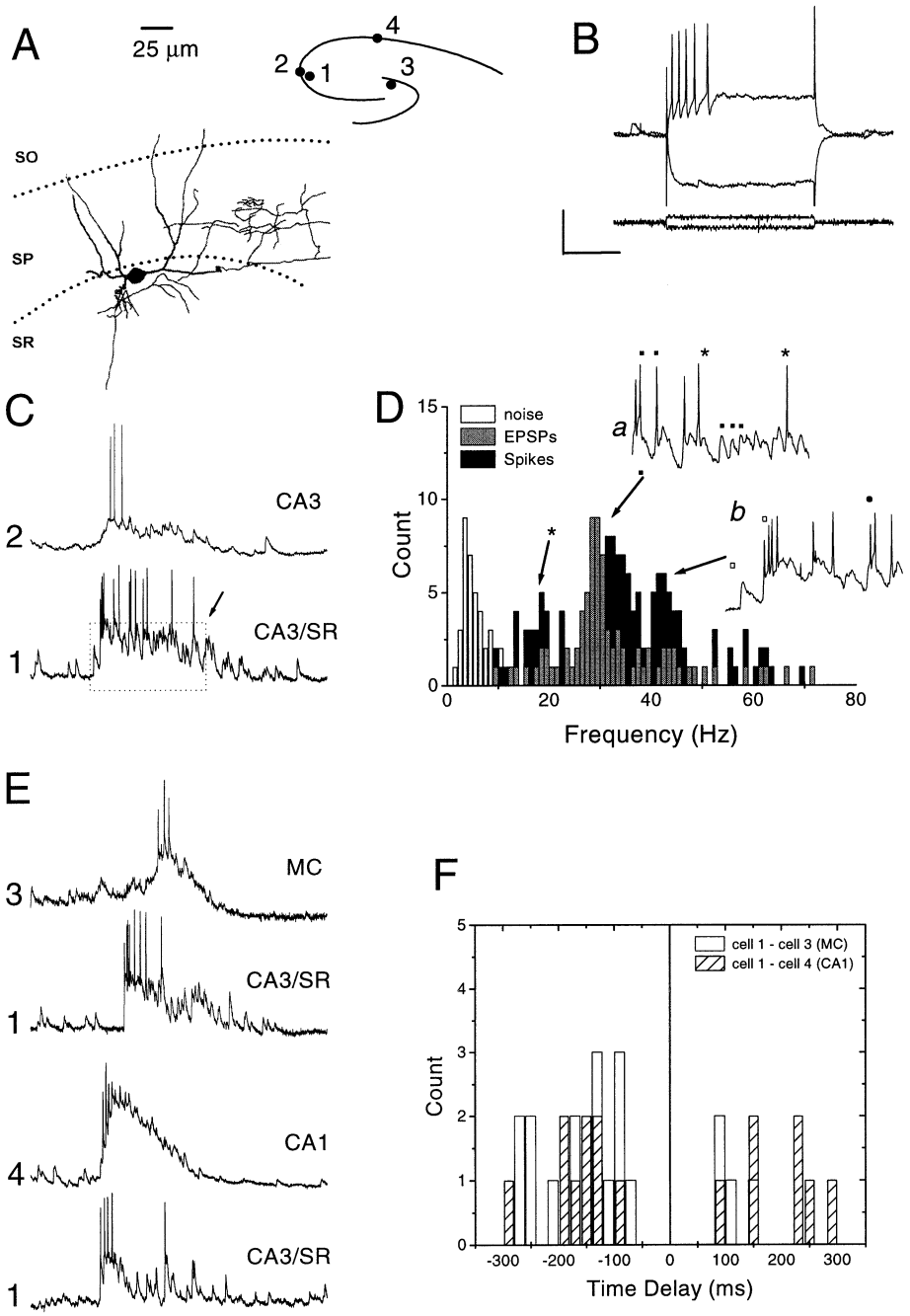

Fig. 4. Properties of the interneuronal firing pattern during GDPs. (A) Camera Lucida drawing of a CA3 interneuron (CA3/SR interneuron). Scale bar = 25 μm. Up: schematic diagram of the position of the four cells shown in this figure. (B) Response of the interneuron shown in A to depolarizing and hyperpolarizing current pulses of ±0.2 nA. (C) Simultaneous recording from the CA3/SR interneuron (cell 1) and a CA3 pyramidal cell (cell 2). See schematic diagram in A. CA3 interneurons fired at high frequency during GDPs. Note also the presence of multiple EPSPs (square). (D) Histograms of the EPSP frequency at background level (noise, white) and of the EPSPs (gray) and spiking (black) in $n = 3$ interneurons during GDPs. (E) Simultaneous recordings from the CA3/SR interneuron (cell 1) and an MC (cell 3). After half an hour of stable recording, a second neuron (at CA1, cell 4) was recorded simultaneously to the CA3/SR interneuron. (F) Time delay histograms of GDPs between the CA3/SR interneuron and MC (white) and CA1 (lines). GDPs were not always initiated from the CA3 interneuron (positive time delays). Calibration bars: 25 mV, 100 ms (B); 25 mV, 250 ms (C, E); 25 mV, 50 ms (inset in D).

appeared after the summation of a given number of EPSPs. Also, every extracellular stimulus induced interneurons to fire, suggesting that there is a coupling between the stimulus frequency and the interneuronal firing frequency. To investigate the possible role of EPSP summation in GDP generation in the interneurons, we estimated the time decay of mossy fiber-mediated EPSPs in comparison to membrane time constants.

By comparing the averaged evoked EPSP with the membrane response to depolarizing current injection, and the voltage dependence of EPSP amplitude, we assessed the electrotonic location of synaptic contacts. In the interneurons, single mossy fiber stimulation evoked EPSPs whose amplitude depended on membrane potential, increasing linearly with hyperpolarization (not shown). The average EPSP and the membrane potential decay showed similar time-courses (Fig. 5D). The mean time constant for the EPSPs was 19.2 ± 2.1 ms (from 40 EPSPs) and the membrane time

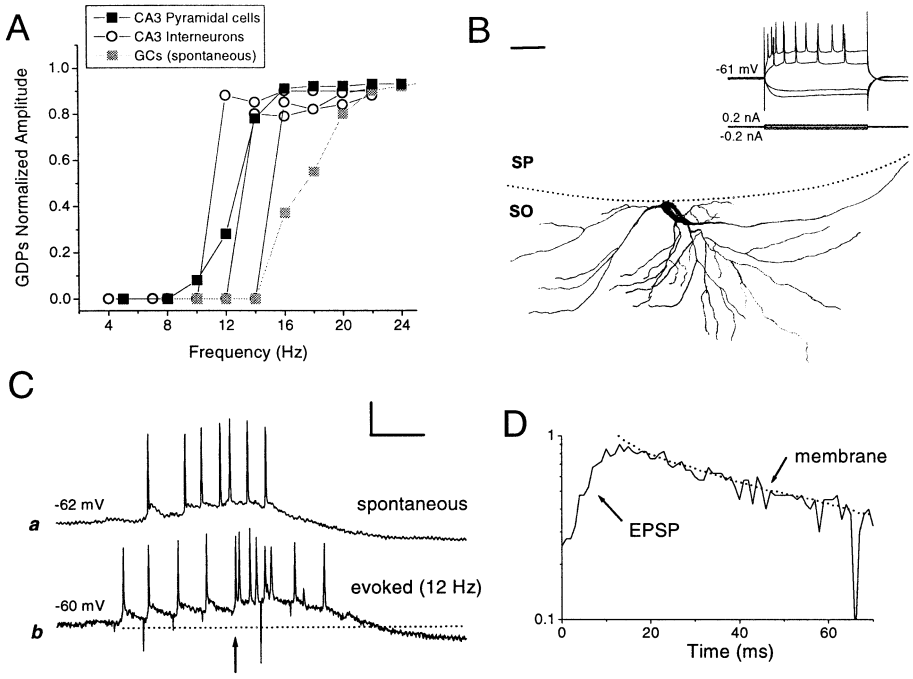

Fig. 5. Frequency dependence of GDP initiation in CA3 interneurons, CA3 pyramidal cells and GCs. (A) Frequency dependence of GDP initiation in interneurons (circles) and CA3 pyramidal cells (squares) investigated by extracellular stimulation of the mossy fibers. GDPs appeared in an all-or-none manner according to stimulus frequency in both interneurons and pyramidal cells. The GDP thresholds were defined at the 50% level of the normalized amplitude, and were 12.5 ± 1.5 Hz (interneurons) and 11.8 ± 2.5 Hz (pyramidal cells). Spontaneous GDPs recorded at GCs also appeared in an all-or-none manner (gray squares). The curve from spontaneous GDP initiation in FD cells was calculated by analysing failures in CA3–GC recordings ($n = 9$). GDP threshold in the FD was at 17 ± 3 Hz. (B) Camera Lucida drawing of a CA3 interneuron with its soma placed at the SO border. Scale bar = 25 μm. Inset: responses to depolarizing and hyperpolarizing current pulses of ± 0.1 and ± 0.2 nA. (C) Spontaneous (trace a) and evoked GDPs (trace b) recorded from the CA3/SO interneuron shown in A. (D) Comparison of the averaged extracellularly evoked EPSP recorded at the interneuron with the membrane response to current injection (+0.1 nA). Calibration bars: 35 mV, 150 ms (B); 35 mV, 250 ms (D).

constant was 20.1 ± 2.8 ms (from 20 trials). All this suggested that synaptic terminals were located near to the recording site (soma).

The role of temporal summation in the initiation of giant depolarizing potentials

Although the frequency-threshold of GDP initiation was similar in both CA3 interneurons and pyramidal cells, some differences were evident. Data from CA3 pyramidal cells ($n = 23$) showed that, in 68% of cases, GDP triggering did not result from EPSP summation. The most common profile of extracellularly evoked GDPs in pyramidal cells was as shown by cell 2 in Fig. 6A, where there is no evidence of temporal summation. In order to quantify the existence of temporal summation prior to a GDP, we used the following criterion: EPSP summation prior to GDPs is present if the onset is masked by EPSP overlap. There were only few CA3 pyramidal cells (13%) in which extracellularly evoked GDPs seemed to be initiated by a summation process, as shown by cell 1 (these two cells were recorded simultaneously). In contrast, in the CA3 interneurons GDPs were more likely to be initiated after EPSP summation and firing. When compared to CA3 pyramidal cells, CA3 interneurons fired more action potentials prior to the onset of the extracellularly evoked GDP (stimulus 0) and EPSPs were more frequent (Fig. 6B).

A different picture was obtained by examining the spontaneous activity. Spontaneously generated GDPs appeared to involve EPSP summation in 32% of CA3 pyramidal cells ($n = 43$) and in only 15% of CA1 pyramidal neurons ($n = 20$). Fifty-seven percent of MCs ($n = 7$) and 53% of GCs ($n = 15$) showed evidence of temporal summation. Nevertheless, in these cases not all the GDPs in a given cell were preceded by EPSP summation: only 43% of GDPs in CA3 cells, 20% in CA1 neurons, 65% in MCs and 31% in GCs. In Fig. 7, we have represented all the cells showing evidence of EPSP summation in more than 30% of the total number of spontaneous GDPs. Those cells showing higher percentages (> 45%) are represented in gray (see trace 1). These results show that EPSP summation was more typically recorded in an area including the hilus, the granule layer and CA3/CA4 region.

Effect of 6-*cyano*-7-*nitroquinoxaline*-2,3-*dione on the onset of giant depolarizing potentials*

The data discussed above do not support that GDPs were initiated by a single population of cells (interneurons, pyramidal or other cellular populations, such as MCs and GCs). Nevertheless, the higher percentages of EPSP summation and firing in the interneurons might suggest a critical role of these cells in GDP generation. If GDPs were determined exclusively by the temporal summation of excitatory GABA-mediated EPSPs, then a blockage of the glutamatergic synaptic transmission should not essentially affect the frequency threshold of GDP onset. To investigate this hypothesis, the selective AMPA/kainate receptor antagonist CNQX (10–20 μM) was applied in rat hippocampal slices from P1 to P6 ($n = 5$; see Experimental Procedures).

Under CNQX, GDPs were still evoked by a frequency-dependent process, although the frequency threshold

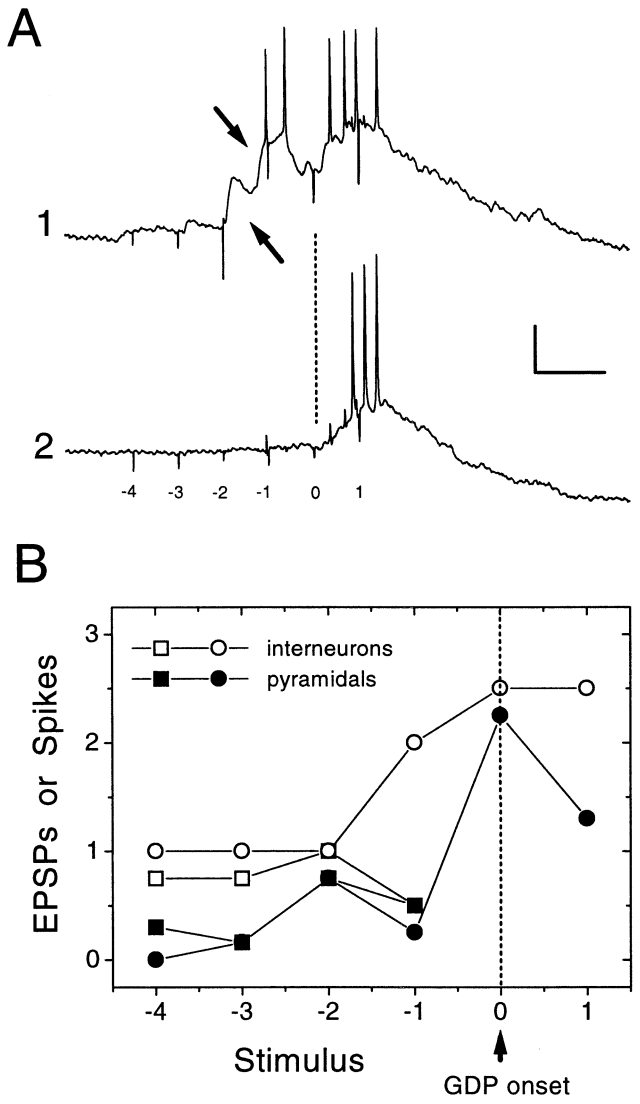

Fig. 6. Electrical activity prior to onset of GDP. (A) Simultaneous recordings from two CA3 pyramidal cells. Extracellular stimulation of suprathreshold frequency was applied. Cell 1 showed evidence of EPSP summation prior to GDP onset (arrows), while cell 2 did not. CA3 pyramidal cells showing EPSP summation constituted 32% of the total. The most common profile of GDP triggering in pyramidal neurons was as shown by cell 2. (B) Comparison of the number of EPSPs (squares) and spikes (circles) evoked by suprathreshold extracellular stimulation in interneurons (white) and pyramidal cells (black). In the interneurons, GDPs were more likely to be initiated after a summation process. Interneurons also fired more action potentials prior to GDP onset (associated to the stimulus 0; see arrow) than pyramidal cells. Calibration bars: 10 mV, 250 ms (A); 8 mV, 100 ms (C); 15 mV, 350 ms (D).

$(47.2 \pm 15.1$ Hz) was significantly higher than in control ($P < 0.001$, $t = 5.7$). Figure 8 illustrates these results. CNQX had a significant effect on the GDPs 9 min after bath application, this effect being maximal after 15 min. The shift of the frequency threshold was reversible (Fig. 8, trace c).

Different capacity of single cells to initiate giant depolarizing potentials

Finally, we tested the ability of different cells to initiate GDPs. We used intracellular depolarizing current pulses injected every 10 s to investigate the entraining capacity of individual neurons. The amplitude of these pulses was fixed so that they evoked firing in the cell. We found no strong evidence of single neurons initiating GDPs; in CA3 IB cells, non-IB cells nor interneurons.

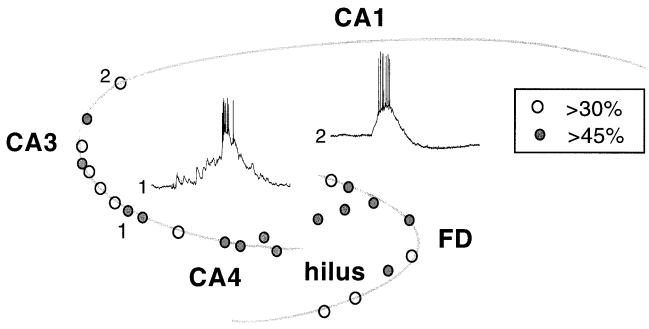

Fig. 7. Schematic representation of the position of cells showing EPSP summation prior to spontaneous GDPs in more that 30% of cases (see trace 1). As can be seen, EPSP summation was more typically recorded at CA3/CA4, the hilus and granule layer. CA1 pyramidal neurons showed the least evidence of EPSP summation (see trace 2). Cells with the highest incidence of EPSP summation are represented in gray.

The results from a non-IB pyramidal cell are shown in Fig. 9A. To evaluate entraining capacity, we calculated the latency between the end of the depolarizing pulse and GDP onset (Fig. 9Ab). We constructed latency histograms from the beginning of a training session (0–400 s) and compared them with those at the end (1200–1600 s; Fig. 9B). As can be seen, there is no significant difference between the histograms from these two situations ($n = 10$ pyramidal cells). On the contrary, one interneuron showed slight differences during the training session, suggesting that this cell could promote GDP initiation (Fig. 9C, D). The CA3/SR interneuron (cell 1) shown in Fig. 4 was tested for entraining capacity while recorded simultaneously with a CA3 pyramidal cell (cell 2). Depolarizing current pulses, injected every 10 s in the CA3/SR interneuron, slightly increased GDP frequency, from 2.9 ± 1.4 GDPs/min in control to 4.2 ± 2.1 GDPs/min, although this difference was not significant ($P > 0.05$, $t = 1.65$). Nevertheless, latency distribution from 0–400 s and 1200–1600 s intervals differed significantly ($P < 0.001$, Mann–Whitney Rank Sum test), showing shorter latencies (0–2 s) 20 min after the initiation of the training session (Fig. 9D, arrow).

In this particular simultaneous recording, small depolarizations of 3.6 ± 0.8 mV in pyramidal cell 2 were detected in association with high-frequency spiking induced by current injection into cell 1 (see traces in Fig. 9C). Since there was no evidence of synaptic contacts from interneuron 1 onto pyramidal cell 2, these results suggest that synaptic terminals from the interneuron may diverge on several cells which then converged onto cell 2 (Fig. 9C, schematic diagram). In these cells, GDPs were also preceded by synchronous EPSPs (arrow), suggesting the presence of divergent connections onto cells 1 and 2. Such a divergence and convergence pattern may be the network support for this interneuronal ability to promote GDP initiation.

DISCUSSION

The conclusions of the present work can be summarized as follows. (1) GDPs are not initiated by a single pacemaker neuronal population, they rather involve the participation of heterogeneous cellular populations which contribute differently

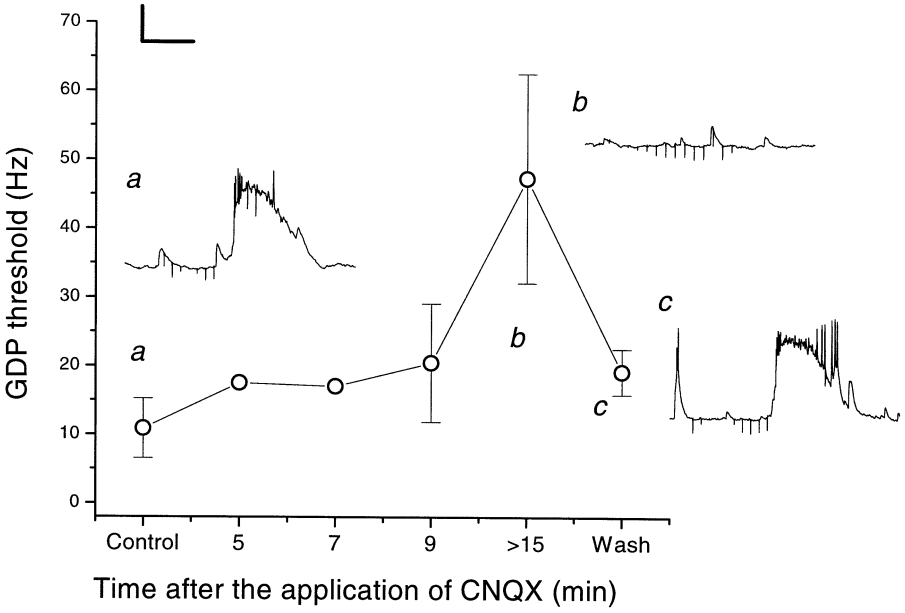

Fig. 8. Effects of CNQX (10–20 μM) in the threshold of frequency for GDP onset. These experiments were conducted in rats (P1–P6). No differences in GDPs were detected between rats and rabbits. GDP threshold was calculated at control, 5, 7, 9 and >15 min of bath application of CNQX. Wash was also examined. Data from $n = 5$ different slices. The traces show the effect of 17-Hz stimulation in three different situations. Trace a: control; trace b: after 15 min of CNQX application; trace c: wash. GDP threshold increased up to 50 Hz after CNQX application. Calibration bars: 25 mV, 200 ms.

according to their intrinsic electrical activity. (2) GDP latency between regions is long and does not depend on the initiation site, being 244 ± 40 ms between FD and CA3, and 208 ± 32 ms between CA3 and CA1. (3) CA3 interneurons do not always initiate GDPs, although they participate in their propagation by firing at high frequency (12–45 Hz). (4) GDP onset takes place in an all-or-none frequency-dependent manner, both spontaneously or when triggered by extracellular stimulation. The threshold of frequency of GDP onset is 17 Hz in granule cells from the FD and 12 Hz in both CA3 pyramidal cells and interneurons. (5) CNQX application increases the threshold of frequency of CA3 pyramidal cells for GDP generation up to 50 Hz. (6) Single cells (IB and non-IB pyramidal cells and interneurons) are unable to entrain GDPs, supporting the view of a cooperative interaction underlying these population bursts.

Intrinsic neuronal activity and recurrent loops underlie the generation of giant depolarizing potentials

Our results support the idea that different neuronal population participate in GDP generation. Experimental and computational studies have demonstrated that recurrent excitation is one of the key factors required for the generation of synchronized network discharges.[68,76,77] In immature hippocampal circuitry, such a recurrent excitation is enhanced by interneuronal networks showing excitatory action via $GABA_A$ receptors.[11] The results obtained from the sliding cross-correlograms showed that GDPs were not originated by a single cellular population; instead, they can be initiated either from CA1, CA3 or FD cells, showing comparable latencies between regions (200 ms). Hippocampal excitatory circuitry is typically unidirectional, from the FD to CA3 and CA1. However, since GDPs involve the synchronous firing of GABAergic interneurons,[31] there is no morphological limitation to their local origin and bidirectional propagation.[8,35,84] Sliding cross-correlograms from CA3–FD recordings showed evidence of recurrent excitatory events among cells from these two areas (detected as double peaks of the cross-correlation function; see Fig. 1B). Previous studies give morphological support to this result by revealing patterns of polysynaptic excitation of GCs by CA3 pyramidal neurons.[55,56] It is shown that there is a glutamatergic AMPA/kainate excitatory pathway from area CA3 to the dentate gyrus in disinhibited hippocampal slices,[54] and a positive feedback between GCs and MCs.[29] It is likely that the operation of these polysynaptic feedback loops depends critically on the strength of excitatory synaptic transmission, which is enhanced in immature networks by the lack of inhibition through $GABA_A$ receptors.

The other principle underlying *in vitro* seizure-like discharges is the intrinsic ability of individual cells to provide background levels of rhythmicity. Our data showed evidence of the intrinsic rhythmic capability of different neuronal populations. As in adults, we found a subpopulation of CA3 pyramidal cells (40%) that fire intrinsic bursts depending on membrane potentials[39,82] (IB cells). IB activity is present in 47% of cases 300 ms prior to GDP onset concomitantly with EPSPs, suggesting its contribution to network synchronization. In fact, IB cells have been shown to be able to locally coordinate synchronous EPSPs/inhibitory postsynaptic potentials in the neocortex even in the presence of strong synaptic inhibition,[9] while in disinhibited hippocampal slices IB cells can entrain the entire CA3 population by means of excitatory recurrent connections.[46,47,61]

We also found a small subset of pyramidal neurons (12%) that did not show stereotyped responses to current pulses but fired spontaneously at 3–10 Hz. Other neuronal populations also showed diverse levels of intrinsic rhythmic activity: immature GCs show poor spontaneous activity and no bursting firing as in the adult,[19] while MCs have higher levels of spontaneous synaptic and firing activity,[57] and were able to fire bursts either spontaneously or in response to current injection, similar to CA3 IB pyramidal cells. A role of MCs during

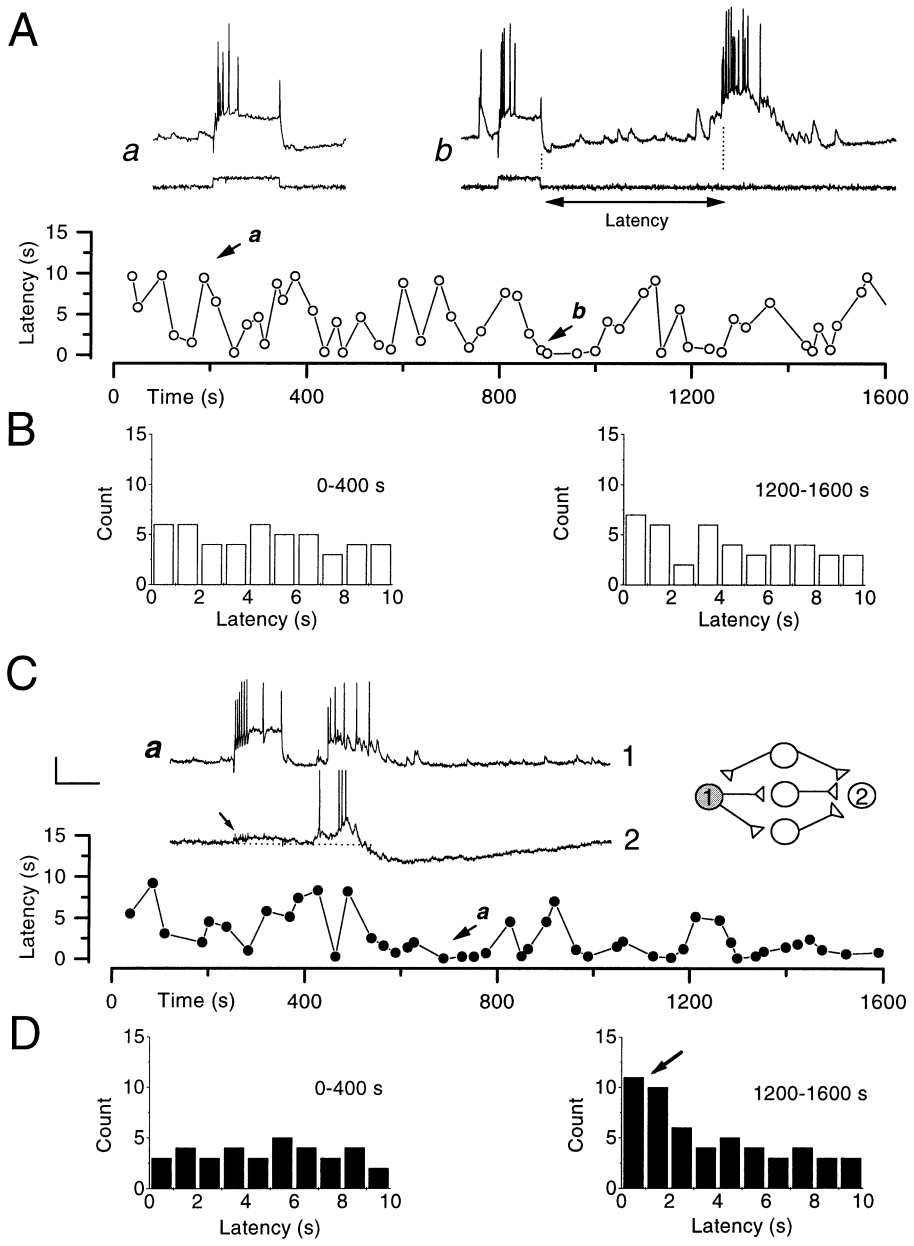

Fig. 9. Analysis of the capability of individual cells to initiate GDPs. (A) Results from a non-IB pyramidal cell. Training protocol consisted of the application of depolarizing current pulses every 10 s for 30 min (a). The latency between the end of the depolarizing pulse and the GDP onset was calculated (b) to evaluate the entraining capacity of the cells. If a single cell is able to initiate GDPs, shorter latencies are expected by the end of the training protocol. (B) Histograms from the beginning of the training session (0–400 s) were compared with histograms from the end (1200–1600 ms). We found no strong evidence of single neurons being able to initiate GDPs, neither CA3 IB pyramidal cells nor non-IB cells. (C) Only one interneuron (the CA3/SR interneuron shown in Fig. 4A) showed a slight difference during the training session, i.e. shorter latencies and a different histogram distribution. (D) Latency histograms at the beginning and end of the training session for this particular interneuron. Calibration bars: 25 mV, 300 ms.

theta oscillation has been reported, supporting their contribution to phase-lock postsynaptic neurons.[62]

Interneurons from this study had a heterogeneous tendency to show spontaneous activity from silent to near 2 Hz, although they exhibit high-frequency spiking during GDPs. In the adult hippocampus, rhythmic activation at 1–8 Hz of presynaptic basket interneurons instantly phase-locks firing in postsynaptic pyramidal neurons.[12] Since a single basket cell is estimated to contact hundreds of pyramidal cells[60] and a pyramidal cell may excite a similar number of inhibitory neurons,[35] it is suggested that feedback loops provide network substrates for the spreading of synchronization.[18,37,72] The hilar inhibitory circuit, for example, is composed of three different subpopulation of GABAergic cells that become synchronized in the absence of glutamate-mediated transmission.[17,45] Within the CA3 and CA1 areas, synaptic recurrent connections among interneurons and pyramidal cells induce interneurons to fire doublets of action potentials (as also shown here in Fig. 4D). These doublets play a key role in synchronizing pyramidal cells at gamma frequencies.[63,75] Therefore, the capacity of interneuronal networks to self-sustain synchronous activity is supported.[5,32,80]

Nevertheless, using whole-cell recordings with electrodes containing fluoride (to block $GABA_A$ receptor-mediated responses), the glutamatergic component of GDPs has been revealed.[4,34] Bath application of CNQX completely blocks

spontaneous GDPs, which are re-induced by the application of GABA, AMPA or by extracellular stimulation. This re-induction is abolished by the more potent AMPA antagonist GYKI 53655, suggesting that their generation requires the activation of AMPA receptors.[4] An NMDA contribution is also suggested, since extracellularly evoked GDPs in the presence of CNQX are blocked by addition of 2-amino-5-phosphonovaleric acid.[31] In all these cases, re-induced GDPs can be completely abolished by bicuculline. Therefore, the generation of GDPs in immature hippocampal networks requires the glutamatergic drive onto the interneurons, and a synergistic activation of $GABA_A$, NMDA and AMPA receptors.[2,20,26] The view of a single population of cells mediating GDPs should thus be discarded. The results discussed here do not support the idea that single neurons could initiate GDPs in the immature hippocampus, although entraining capability has been demonstrated in disinhibited adult slices[46] and in juvenile hippocampal slices (P9–P16) exposed to convulsants.[23,61]

The local hypothesis

Our results help to understand how synchrony develops in immature hippocampal networks. (1) Rhythmic intrinsic activity in one cell, such as IB cells or rhythmically spiking neurons, can be transmitted to postsynaptic cells by divergent patterns of connections (Figs 2C, 3D, E). (2) Several neurons could share common inputs from different presynaptic cells (Fig. 3D). This divergence/convergence enhances the recruitment of a local population of GABAergic and glutamatergic neurons. (3) Recurrent connections guarantee the reverberation of synchronous local activity and the development of a full synchronous firing pattern, i.e. GDPs. Prior to full synchronization, there is a build up period (integration period), lasting from 100 to 300 ms, in which synchronous EPSPs and action potentials can be recorded (Fig. 1D; also see Figs 1A and 2A in Ref. 43). This synchronous activity reflects the growth of firing in an initial group of cells, which subsequently spread by increasing the number of neurons recruited. Integration periods preceding population bursts are present not only in hippocampal networks under high potassium,[10,70] but also in other cortical preparations[7,16,25] and spinal networks.[49] In the case of GDPs, the duration of the integration period is long and highly variable for a given cell pair, suggesting that GDPs are not always generated by the same cellular groups. This is particular evident in sliding cross-correlograms which show heterogeneous profiles of temporal dependency (Fig. 1B). (4) After the integration period, full synchronization, and therefore a GDP, appears in an all-or-none manner depending on the EPSP frequency in the recruited cells (Fig. 5A). The frequency threshold appears to be a network property, since it could be modified by a pharmacological tuning of synaptic interactions (Fig. 8), which differs depending on the networks, such as CA3 and the FD.[43,44]

Based on these results, a local hypothesis of the origin of GDPs can be proposed. The local hypothesis is supported by data from CA3, CA1 and FD minislices where GDPs are still recorded.[41] In this view, full synchronization in immature hippocampal networks originates locally from a heterogeneous population of intrinsically active neurons (GABAergic and glutamatergic) which are densely connected. The rate and extent of synaptic connections, together with the intrinsic rhythmic capability, would determine the capacity of a given "cluster" of neurons to act as a GDP focus. This implies a different capacity of hippocampal regions to generate GDPs, the CA3 area being the most outstanding.[31] Interneurons are essential in the development of this synchrony, since their excitatory effect via $GABA_A$ receptors enhances the synaptic activity and chloride currents are the main component of GDPs.[4] In fact, $GABA_A$ receptors appear to be the principal pathway of synaptic transmission in the developing hippocampus, since the majority of spontaneous EPSPs are blocked by bicuculline.

The frequency threshold of synchronization as a network property

Synchronization is present in brain activity associated with perception, encoding or processing, and occurs at particular frequencies depending on the networks and the rhythmic capacity of the component cells.[15,30,66,38,67] The CA3 synchronization threshold of 12 Hz is dependent on synaptic connections, since it is modified by CNQX application (Fig. 8). When compared, CA3 and FD networks show different thresholds for GDP generation, i.e. 12 and 17 Hz, respectively (Fig. 5A). Such a difference is evident in the lower occurrence of GDPs reported from the FD[43] and could also be the basis for the filtering capability of the dentate gyrus during seizures.[22,36,52] The connectivity difference between the CA3 area and the FD is widely documented.[6,81] Nevertheless, there is an alternative explanation, since the FD threshold was calculated from spontaneous activity (based on the high failure incidence: ~10%), while the CA3 threshold was investigated using extracellular stimulation (since CA3 showed a small failure percentage: ~2%). Perhaps one source of discrepancy between the spontaneous and forced results was in the interactions between the input pulses[3] or the massive stimulation of mossy terminals, a situation that is not present spontaneously. Nevertheless, when isolated, CA3 networks show higher GDP incidence than the isolated FD,[41] suggesting a higher synchronizing capability of immature CA3 circuitry based on its high connectivity.[35] However, the question still remains: which mechanism would explain where the 12- or 17-Hz threshold comes from?

In CA3 interneurons, the 12-Hz frequency threshold for full synchronization within CA3 networks appears to be similar to the frequency of evoked EPSPs prior to GDP onset (Fig. 5C, trace b). This might suggest that temporal summation in the interneurons would underlie the frequency dependence of the GDP initiation process.[7] Nevertheless, blockage of synaptic transmission via AMPA/kainate receptors increases the threshold of frequency, which suggests that such a threshold is not imposed by interneuronal activity. On the other hand, we found a mean time constant of 19 ms in the CA3 interneurons, which would support a frequency of synchronization of about 50 Hz (under the criterion that summation of GABA-mediated EPSPs occurs at one time constant). Interestingly, this was the frequency threshold detected when glutamatergic transmission was reduced by CNQX application. The frequency threshold of 12 Hz determines an 80-ms time interval between successive pulses for temporal summation. CA3 interneurons and pyramidal cells in this study showed a membrane time constant of nearly 20 ms (see Table 1 and Ref. 43). This implies that at least four postsynaptic potentials can be summed within one time interval of 12-Hz

synchronization (4×20 ms $= 80$ ms $\rightarrow 12$ Hz). Since full synchronization requires the synergistic activation of $GABA_A$, NMDA and AMPA receptors, it is expected that the summed postsynaptic potential should contain these three components; 12 Hz may thus be representing the minimal number of EPSPs required for synergistic cooperation. Nevertheless, attention must be paid not only to the membrane time constant, but also to the time-course of particular receptors. Experimental and computational studies have shown a relationship between the frequency of network oscillations and the decay time constant in cell-to-cell connections.[75,80] A possible analytical explanation of the 12-Hz frequency threshold arises from detailed data on EPSP–receptor kinetics from different immature cellular groups or even from different subsets of interneurons.[27,50]

As illustrated in Fig. 7, few pyramidal cells (32%) might support evidence of temporal summation. CA1 pyramidal cells, MCs and GCs also showed evidence of EPSP summation to different extents. In all cases, not all the GDPs in a given cell were preceded by EPSP summation, which suggests an alternative explanation, i.e. temporal summation effectively underlies the frequency threshold mechanism, but this would only be detectable near to the GDP initiation sites. Results in other preparations, such as the piriform cortex, support this idea.[25] By drawing the position of all the cells showing the highest levels of EPSP summation (>30%), we found that the region including the hilus, the granule layer and CA3/CA4 area is most likely to initiate GDPs. In this view, GDPs are initiated locally by an all-or-none mechanism depending on EPSP summation beyond a threshold of frequency. The position of these initiation sites does not appear to be fixed; instead, a dynamic picture can be proposed based on the variability of the integration period preceding GDP onset. Imaging experiments may help to elucidate this alternative.[13,79]

Acknowledgements—This work was supported by grant 96/2012 from the FIS. L.M.P. was supported by a Posdoctoral Fellowship from Generalitat Valenciana and Comunidad de Madrid. We thank S.Bolea for the experiments with CNQX and useful comments. We also thank O. Herreras for careful reading of the manuscript and helpful discussions.

REFERENCES

1. Ben-Ari Y., Cherubini E., Corradetti R. and Gaiarsa J. L. (1989) Giant synaptic potentials in immature rat CA3 hippocampal neurones. *J. Physiol.* **416,** 303–325.
2. Ben-Ari Y., Khazipov R., Leinekugel X., Caillard O. and Gaiarsa J. L. (1997) $GABA_A$, NMDA and AMPA receptors: a developmentally regulated "ménage a trois". *Trends Neurosci.* **20,** 523–529.
3. Berger T. W., Eriksson J. L., Ciarolla D. A. and Sclabassi R. J. (1998) Nonlinear systems analysis of the hippocampal perforant path–dentate projection. II. Effects of random impulse train stimulation. *J. Neurophysiol.* **60,** 1077–1094.
4. Bolea S., Avignone E., Berretta N., Sanchez-Andres J. V. and Cherubini E. (1999) Glutamate controls the induction of GABA-mediated giant depolarising potentials through AMPA receptors in neonatal rat hippocampal slices. *J. Neurophysiol.* **81,** 2095–2102.
5. Buzsaki G., Horvath Z., Urioste R., Hetke J. and Wise K. (1992) High-frequency network oscillation in the hippocampus. *Science* **256,** 1025–1027.
6. Caeser M. and Aertsen A. (1991) Morphological organization of rat hippocampal slice cultures. *J. comp. Neurol.* **307,** 87–106.
7. Calvin W. H. (1972) Synaptic potential summation and repetitive firing mechanisms: input–output theory for the recruitment of neurons into epileptic bursting firing patterns. *Brain Res.* **39,** 71–94.
8. Ceranik K., Bender R., Geiger J. R. P., Monyer H., Jonas P., Frotscher M. and Lübke J. (1997) A novel type of GABAergic interneuron connecting the input and the output regions of the hippocampus. *J. Neurosci.* **17,** 5380–5394.
9. Chagnac-Amitai Y. and Connors B. W. (1989) Synchronized excitation and inhibition driven by intrinsically bursting neurons in neocortex. *J. Neurophysiol.* **62,** 1149–1162.
10. Chamberlin N. L., Traub R. D. and Dingledine R. (1990) Role of EPSPs in initiation of spontaneous synchronized burst firing in rat hippocampal neurons bathed in high potassium. *J. Neurophysiol.* **64,** 1000–1008.
11. Cherubini E., Gaiarsa J. L. and Ben Ari Y. (1991) GABA: an excitatory transmitter in early postnatal life. *Trends Neurosci.* **14,** 515–519.
12. Cobb S. R., Buhl E. H., Halasy K., Paulsen O. and Somogyi P. (1995) Synchronization of neuronal activity in hippocampus by individual GABAergic interneurons. *Nature* **378,** 75–78.
13. Colom L. V. and Saggau P. (1994) Spontaneous interictal-like activity originates in multiple areas of the CA2–CA3 region of hippocampal slices. *J. Neurophysiol.* **71,** 1574–1585.
14. Connors B. W. and Gutnick M. J. (1990) Intrinsic firing patterns of diverse neocortical neurons. *Trends Neurosci.* **13,** 99–104.
15. Contreras D., Destexhe A., Sejnowski T. J. and Steriade M. (1997) Spatiotemporal pattern of spindle oscillations in cortex and thalamus. *J. Neurosci.* **17,** 1179–1196.
16. Demir R., Haberly L. B. and Jackson M. B. (1999) Sustained and accelerating activity at two discrete sites generates epileptiform discharges in slices of piriform cortex. *J. Neurosci.* **19,** 1294–1306.
17. Forti M. and Michelson H. B. (1998) Synaptic connectivity of distinct hilar interneuron subpopulations. *J. Neurophysiol.* **79,** 3229–3237.
18. Freund T. F. and Buzsáki G. (1996) Interneurons of the hippocampus. *Hippocampus* **6,** 347–470.
19. Fricke R. A. and Prince D. A. (1984) Electrophysiology of dentate gyrus granule cells. *J. Neurophysiol.* **51,** 195–209.
20. Gaiarsa J. L., Corradetti R., Ben Ari Y. and Cherubini E. (1990) GABA mediated synaptic events in neonatal rat CA3 pyramidal neurons *in vitro*: modulation by NMDA and non-NMDA receptors. *Adv. exp. Med. Biol.* **268,** 151–159.
21. Garaschuk O., Hanse E. and Konnerth A. (1998) Developmental profile and synaptic origin of early network oscillations in the CA1 region of rat neonatal hippocampus. *J. Physiol.* **507,** 219–236.
22. Gloveli T., Schmitz D., Empson R. M. and Heinemann U. (1997) Frequency-dependent information flow from the entorhinal cortex to the hippocampus. *J. Neurophysiol.* **78,** 3444–3449.
23. Gomes di Cesare C. M., Smith K. L., Rice F. L. and Swann J. W. (1996) Anatomical properties of fast spiking cells that initiate synchronized population discharges in immature hippocampus. *Neuroscience* **75,** 83–97.
24. Hablitz J. J. (1984) Picrotoxin-induced epileptiform activity in the hippocampus: role of endogenous versus synaptic factors. *J. Neurophysiol.* **51,** 1011–1027.
25. Hoffman W. H. and Haberly L. B. (1993) Role of synaptic excitation in the generation of bursting-induced epileptiform potentials in the endopiriform nucleus and piriform cortex. *J. Neurophysiol.* **70,** 2550–2561.
26. Hollrigel G. S., Ross S. T. and Soltesz I. (1998) Temporal patterns and depolarizing actions of spontaneous GABAA receptor activation in granule cells of the early postnatal dentate gyrus. *J. Neurophysiol.* **80,** 2340–2351.
27. Hollrigel G. S. and Soltesz I. (1997) Slow kinetics of miniature IPSCs during early postnatal development in granule cells of the dentate gyrus. *J. Neurosci.* **17,** 5119–5128.

28. Ives A. E. and Jefferys J. G. R. (1990) Synchronization of epileptiform bursts induced by 4-aminopyridine in the *in-vitro* hippocampal slice preparation. *Neurosci. Lett.* **112,** 239–245.
29. Jackson M. B. and Scharfman H. E. (1996) Positive feedback from hilar mossy cells to granule cells in the dentate gyrus revealed by voltage-sensitive dye and microelectrode recording. *J. Neurophysiol.* **76,** 601–616.
30. Jefferys J. G. R., Traub R. D. and Whittington M. A. (1996) Neuronal networks for induced "40 Hz" rhythms. *Trends Neurosci.* **19,** 202–208.
31. Khazipov R., Leinekugel X., Khalilov I., Gaiarsa J. L. and Ben-Ari Y. (1997) Synchronization of GABAergic interneuronal network in CA3 subfield of neonatal rat hippocampal slices. *J. Physiol.* **498,** 763–772.
32. Lacaille J. C., Mueller A. L., Kunkel D. D. and Schwartzkroin P. A. (1987) Local circuit interaction between oriens/alveus interneurons and CA1 pyramidal cells in hippocampal slices: electrophysiology and morphology. *J. Neurosci.* **7,** 1979–1993.
33. Laurent G. and Davidowitz H. (1994) Encoding of olfactory information with oscillating neural assemblies. *Science* **265,** 1872–1875.
34. Leinekugel X., Medina I., Khalilov I., Ben-Ari Y. and Khazipov R. (1997) Ca^{2+} oscillations mediated by the synergistic excitatory actions of $GABA_A$ and NMDA receptors in the neonatal hippocampus. *Neuron* **18,** 243–255.
35. Li X. G., Somogyi P., Ylinen A. and Buzsaki G. (1997) The hippocampal CA3 network: an *in vivo* intracellular labeling study. *J. comp. Neurol.* **339,** 181–208.
36. Lothman E. W., Stringer J. L. and Bertram E. H. (1992) The dentate gyrus as a control point for seizures in the hippocampus and beyond. *Epilepsy Res., Suppl.* **7,** 301–313.
37. Lytton W. W. and Sejnowski T. J. (1991) Simulations of cortical pyramidal neurons synchronized by inhibitory interneurons. *J. Neurophysiol.* **66,** 1059–1079.
38. Marino J., Martinez L. and Canedo A. (1996) Coupled slow and delta oscillations between cuneothalamic and thalamocortical neurons in the chloralose anesthetized cat. *Neurosci. Lett.* **219,** 107–110.
39. Masukawa L. M., Benardo L. S. and Prince D. A. (1982) Variations in electrophysiological properties of hippocampal neurons in different subfields. *Brain Res.* **242,** 341–344.
40. Menendez de la Prida L., Bolea S. and Sanchez-Andres J. V. (1996) Analytical characterization of spontaneous activity evolution during hippocampal development in the rabbit. *Neurosci. Lett.* **218,** 185–187.
41. Menendez de la Prida L., Bolea S. and Sanchez-Andres J. V. (1998) Origin of the synchronized network activity in the rabbit developing hippocampus. *Eur. J. Neurosci.* **10,** 899–906.
42. Menendez de la Prida L. and Sanchez-Andres J. V. (1998) Local mechanisms underlying synchronized activity in developing hippocampus. *J. Physiol.* **509P,** 68.
43. Menendez de la Prida L. and Sanchez-Andres J. V. (1999) Non-linear frequency-dependent synchronization in the developing hippocampus. *J. Neurophysiol.* **82,** 202–208.
44. Menendez de la Prida L. and Sanchez-Andres J. V. (1999) Nonlinear transfer function encodes synchronization in a neural network from the mammalian brain. *Phys. Rev. E* **60,** 3239–3243.
45. Michelson H. B. and Wong R. K. S. (1994) Synchronization of inhibitory neurones in the guinea-pig hippocampus *in vitro. J. Physiol., Lond.* **477,** 35–45.
46. Miles R. and Wong R. K. S. (1983) Single neurones can initiate synchronized population discharge in the hippocampus. *Nature* **306,** 371–373.
47. Miles R. and Wong R. K. S. (1987) Inhibitory control of local excitatory circuits in the guinea-pig hippocampus. *J. Physiol.* **388,** 611–629.
48. Miles R., Wong R. K. S. and Traub R. D. (1984) Synchronized afterdischarges in the hippocampus: contribution of local synaptic interactions. *Neuroscience* **12,** 1179–1189.
49. O'Donovan M. J. (1999) The origin of spontaneous activity in developing networks of the vertebrate nervous system. *Curr. Opin. Neurobiol.* **9,** 94–104.
50. Parra P., Gulyás A. I. and Miles R. (1998) How many subtypes of inhibitory cells in the hippocampus? *Neuron* **20,** 983–993.
51. Press W. H., Teukolsky S. A., Vetterling W. T. and Flannery B. P. (1992) *Numerical Recipes in C: The Art of Scientific Computing*. Cambridge University Press, Cambridge.
52. Scharfman H. E. (1991) Dentate hilar cells with dendrites in the molecular layer have lower thresholds for synaptic activation by perforant path than granule cells. *J. Neurosci.* **11,** 1660–1673.
53. Scharfman H. E. (1994) Evidence from simultaneous intracellular recordings in rat hippocampal slices that area CA3 pyramidal cells innervate dentate hilar mossy cells. *J. Neurophysiol.* **72,** 2167–2180.
54. Scharfman H. E. (1994) Synchronization of area CA3 hippocampal pyramidal cells and non-granule cells of the dentate gyrus in bicuculline-treated rat hippocampal slices. *Neuroscience* **59,** 245–257.
55. Scharfman H. E. (1996) Conditions required for polysynaptic excitation of dentate granule cells by area CA3 pyramidal cells in rat hippocampal slices. *Neuroscience* **72,** 655–668.
56. Scharfman H. E., Kunkel D. D. and Schwartzkroin P. A. (1990) Synaptic connections of dentate granule cells and hilar neurons: results of paired intracellular recordings and intracellular horseradish peroxidase injections. *Neuroscience* **37,** 693–707.
57. Scharfman H. E. and Schwartzkroin P. A. (1988) Electrophysiology of morphologically identified mossy cells of the dentate hilus recorded in guinea pig hippocampal slices. *J. Neurosci.* **8,** 3812–3821.
58. Schwartzkroin P. A. (1982) Development of rabbit hippocampus: physiology. *Devl Brain Res.* **2,** 469–486.
59. Schwartzkroin P. A., Moshé S. L., Noebels J. L. and Swann J. W. (1995) *Brain Development and Epilepsy*. Oxford University Press, Oxford.
60. Sik A., Penttonen M., Ylinen A. and Buzsáki G. (1995) Hippocampal CA1 interneurons: an *in vivo* intracellular labeling study. *J. Neurosci.* **15,** 6651–6665.
61. Smith K. L., Szarowski D. H., Turner J. N. and Swann J. W. (1995) Diverse neuronal populations mediate local circuit excitation in area CA3 of developing hippocampus. *J. Neurophysiol.* **74,** 650–672.
62. Soltesz I. and Deschenes M. (1993) Low- and high-frequency membrane potential oscillations during theta activity in CA1 and CA3 pyramidal neurons of the rat hippocampus under ketamine–xylazine anesthesia. *J. Neurophysiol.* **70,** 97–116.
63. Stanford I. M., Traub R. D. and Jefferys J. G. R. (1998) Limbic gamma rhythms. II. Synaptic and intrinsic mechanisms underlying spike doublets in oscillating subicular neurons. *J. Neurophysiol.* **80,** 162–171.
64. Strata F., Atzori M., Molnar M., Ugolini G., Tempia F. and Cherubini E. (1997) A pacemarker current in dye-coupled hilar interneurons contributes to the generation of giant GABAergic potentials in developing hippocampus. *J. Neurosci.* **17,** 1435–1446.
65. Swann J. W., Smith K. L. and Brady R. J. (1993) Localized excitatory synaptic interactions mediate the sustained depolarization of electrographic seizures in developing hippocampus. *J. Neurosci.* **13,** 4680–4689.
66. Timofeev I. and Steriade M. (1996) Low-frequency rhythms in the thalamus of intact-cortex and decorticated cats. *J. Neurophysiol.* **76,** 4152–4168.
67. Timofeev I. and Steriade M. (1997) Fast (mainly 30–100 Hz) oscillations in the cat cerebellothalamic pathway and their synchronization with cortical potentials. *J. Physiol., Lond.* **504,** (1) 153–168.
68. Traub R. D., Borck C., Colling S. B. and Jefferys J. G. R. (1996) On the structure of ictal events *in vitro*. *Epilepsia* **37,** 879–891.
69. Traub R. D., Colling S. B. and Jefferys J. G. R. (1995) Cellular mechanisms of 4-aminopyridine-induced synchronized after-discharges in the rat hippocampal slice. *J. Physiol., Lond.* **489,** 127–140.
70. Traub R. D. and Dingledine R. (1990) Model of the synchronized epileptiform bursts induced by high potassium in the CA3 region of the rat hippocampal slice: role of spontaneous EPSPs in initiation. *J. Neurophysiol.* **64,** 1009–1018.
71. Traub R. D., Knowles W. D., Miles R. and Wong R. K. S. (1987) Models of the cellular mechanism underlying propagation of epileptiform activity in the CA2–CA3 region of the hippocampal slice. *Neuroscience* **21,** 457–470.

72. Traub R. D. and Miles R. (1991) *Neuronal Networks of the Hippocampus*. Cambridge University Press, Cambridge.
73. Traub R. D., Miles R. and Jefferys J. G. R. (1993) Synaptic and intrinsic conductances shape picrotoxin-induced synchronized after-discharges in the guinea-pig hippocampal slice. *J. Physiol.* **461,** 525–547.
74. Traub R. D., Miles R. and Wong R. K. S. (1989) Model of the origin of rhythmic population oscillations in the hippocampal slice. *Science* **243,** 1319–1325.
75. Traub R. D., Whittington M. A., Colling S. B., Buzsaki G. and Jefferys J. G. R. (1996) Analysis of gamma rhythms in the rat hippocampus *in vitro* and *in vivo*. *J. Physiol., Lond.* **493,** 471–484.
76. Traub R. D., Whittington M. A., Stanford I. M. and Jefferys J. G. R. (1996) A mechanism for generation of long-range synchronous fast oscillations in the cortex. *Nature* **383,** 621–624.
77. Traub R. D. and Wong R. K. S. (1982) Cellular mechanism of neuronal synchronization in epilepsy. *Science* **216,** 745–747.
78. Traub R. D., Wong R. K. S., Miles R. and Michelson H. (1991) A model of a CA3 hippocampal pyramidal neuron incorporating voltage-clamp data on intrinsic conductances. *J. Neurophysiol.* **66,** 635–650.
79. Tsau Y., Guan L. and Wu J. Y. (1998) Initiation of spontaneous epileptiform activity in the neocortical slice. *J. Neurophysiol.* **80,** 978–982.
80. Whittington M. A., Traub R. D. and Jefferys J. G. R. (1995) Synchronized oscillations in interneuron networks driven by metabotropic glutamate receptor activation. *Nature* **373,** 612–615.
81. Witter M. P. (1993) Organization of the entorhinal–hippocampal system: a review of current anatomical data. *Hippocampus* **3,** (Spec. No.) 33–44.
82. Wong R. K. S. and Prince D. A. (1981) Afterpotential generation in hippocampal pyramidal cells. *J. Neurophysiol.* **45,** 86–97.
83. Wuarin J. P. and Dudek F. E. (1996) Electrographic seizures and new recurrent excitatory circuits in the dentate gyrus of hippocampal slices from kainate-treated epileptic rats. *J. Neurosci.* **16,** 4438–4448.
84. Yeckel M. F. and Berger T. W. (1990) Feedforward excitation of the hippocampus by afferents from the entorhinal cortex: redefinition of the role of the trisynaptic pathway. *Proc. natn. Acad. Sci. U.S.A.* **87,** 5832–5836.

(*Accepted* 19 *January* 2000)